DE LA RECHERCHE À L'INDUSTRIE

cea

SHAPE VARIABILITY OF THE CENTRAL SULCUS IN THE DEVELOPING BRAIN: A LONGITUDINAL DESCRIPTIVE AND PREDICTIVE STUDY IN PRETERM INFANTS

NeoBrain 2 | Héloïse de Vareilles

Jessica Dubois, Denis Rivière, Jean-François Mangin, Manon Benders

www.cea.fr

DE LA RECHERCHE À L'INDUSTRIE

cea

I. Context: why study the developing central sulcus?

II. Method: how to capture the shape variability of the central sulcus?

III. Descriptive results: what shape specificities do we observe in the developing central sulcus?

IV. Predictive results: is the developing central sulcus informative about motor outcome at 5 years?

I. Context: why study the developing central sulcus?

II. Method: how to capture the shape variability of the central sulcus?

III. Descriptive results: what shape specificities do we observe in the developing central sulcus?

IV. Predictive results: is the developing central sulcus informative about motor outcome at 5 years?

Why do we study sulci ?

→ **Unique folding patterns for each individual**
→ **Global resemblance within the kin allowing comparison**
→ **Macroscopic proxy for brain development**
→ **Links between cortical folding patterns and functional outcomes**

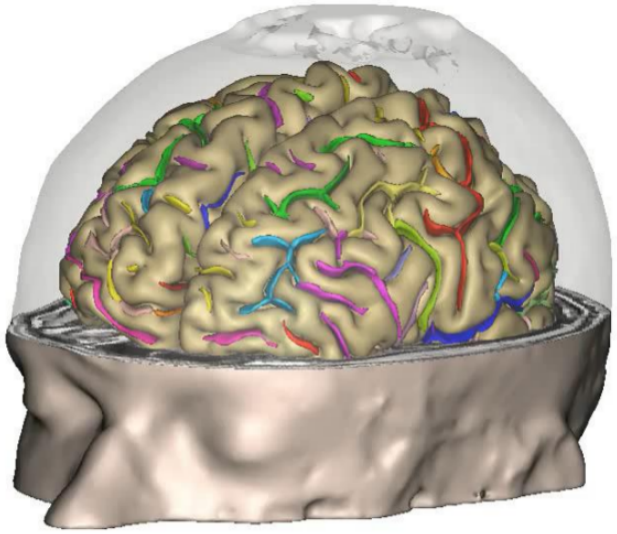

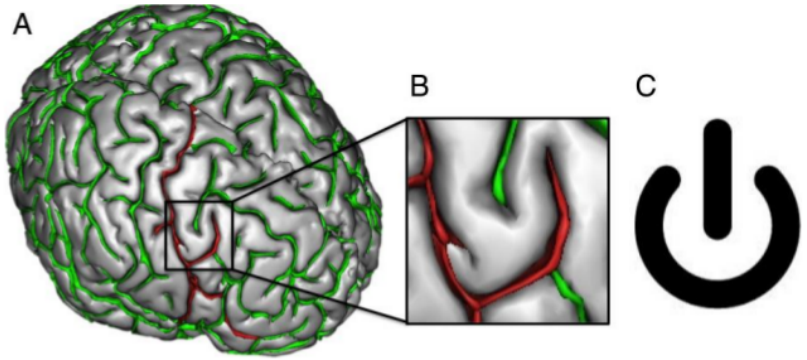

Illustration of the Power Button sign, biomarker for epilepsy [1]

[1] Mellerio et al., Radiolgy, 2015.The Power Button Sign: A Newly Described Central Sulcal Pattern on Surface Rendering MR Images of Type 2 Focal Cortical Dysplasia

Why focus on the central sulcus ?

→ **Simple sulcus, systematic and easy to identify**
→ **Early development**
→ **Link with sensorimotor function established through somatotopic maps [1]**
→ **Shape variability already assessed in the adult [2,3]**

A.

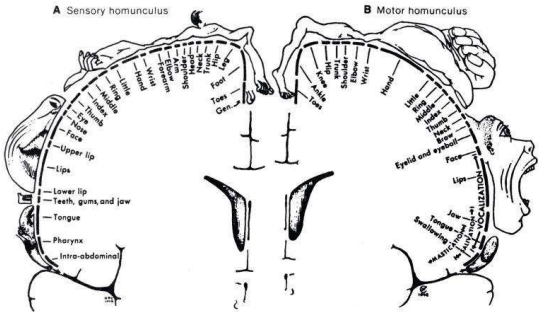

B.

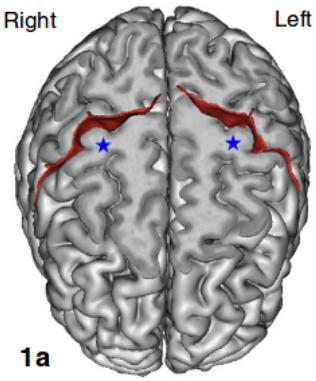

Central sulcus
★hand knob

C.

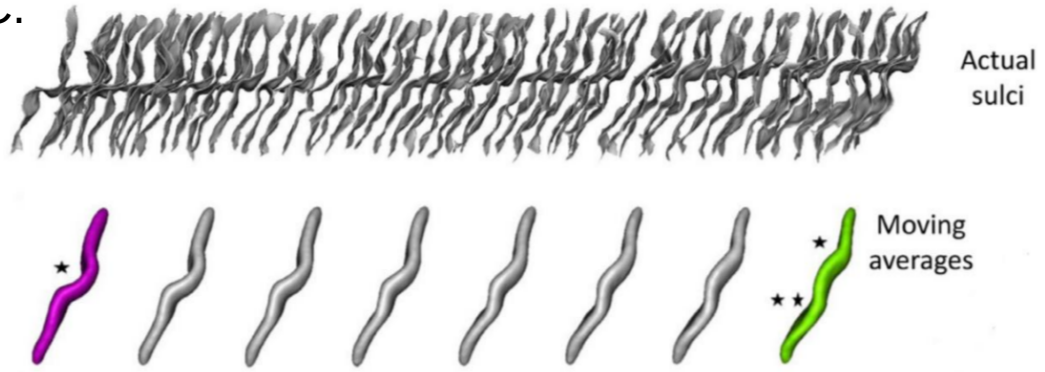

Main variability feature in the adult Central Sulcus [3]

[1] Penfield et Rasmussen, 1950. *The cerebral cortex of man; a clinical study of localization of functions.*
[2] Sun et al., NeuroImage, 2012. The effect of handedness on the shape of the central sulcus
[3] Mangin et al., Medical Image Analysis, 2016. Spatial normalization of brain images and beyond.

Why focusing on preterms ?

→ **Sulci develop mostly during the 3rd trimester of pregnancy**
→ **Longitudinal analyses on fetal MRI are highly complex**
→ **We may capture sulcal specificities of preterm development**

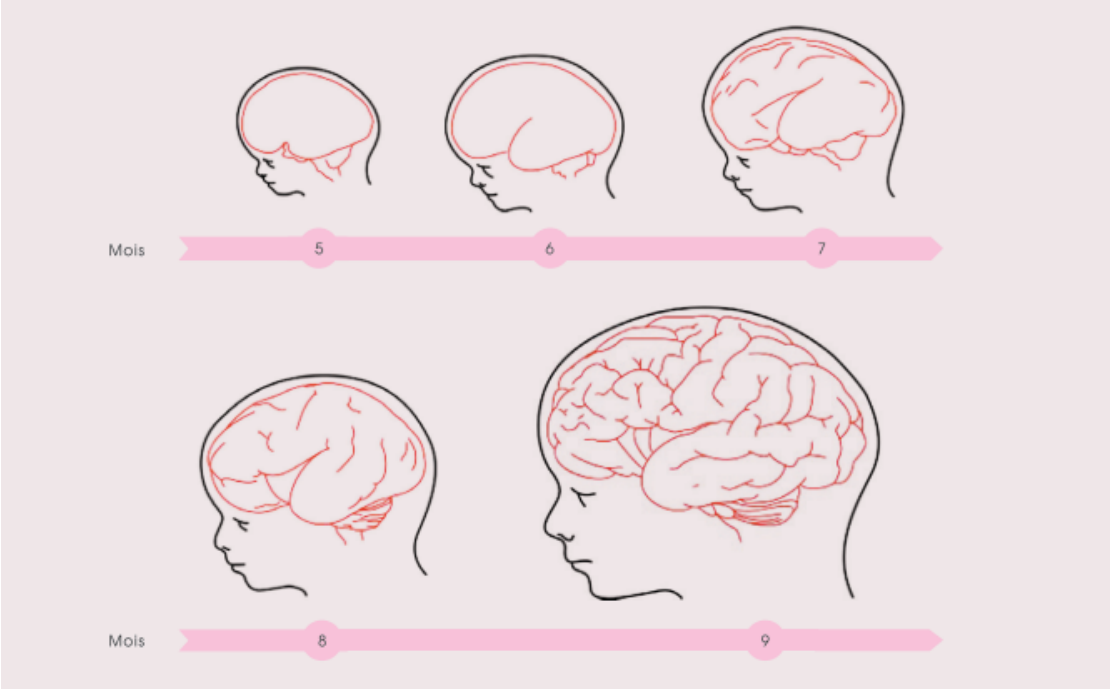

Image courtesy of G. Dehaene and J. Dubois. (*Au tout départ: le c3rv34u du bébé*)

DE LA RECHERCHE À L'INDUSTRIE

cea

I. Context: why study the developing central sulcus?

II. Method: how to capture the shape variability of the central sulcus?

III. Descriptive results: what shape specificities do we observe in the developing central sulcus?

IV. Predictive results: is the developing central sulcus informative about motor outcome at 5 years?

Presentation of the cohort

71 very preterm newborns from Wilhelmina Children's hospital, Utrecht, the Netherlands [1], with a gestational age at birth between 24 and 28 weeks. Age after birth is referred in terms of weeks of post-menstrual age (w PMA)

1st MRI at ~30w PMA (28.7 – 32.7w PMA) → 2nd MRI at ~40w PMA (40 – 42.7w PMA) → Handedness and motor assessment at ~5 years

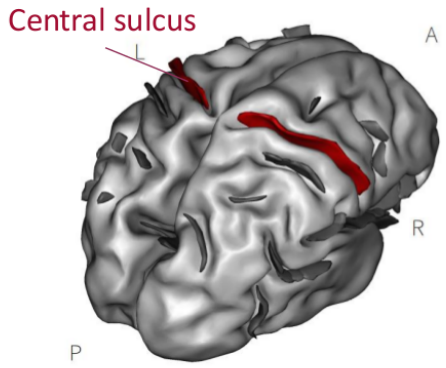

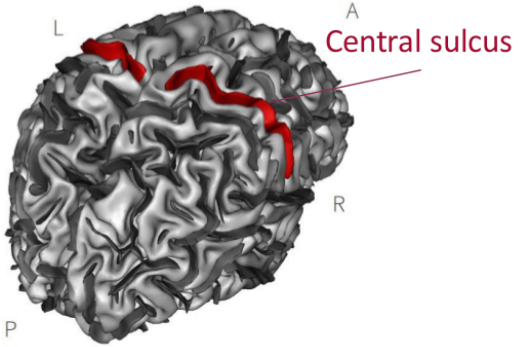

[1] Kersbergen et al., NeuroImage, 2016. Relation between clinical risk factors, early cortical changes, and neurodevelopmental outcome in preterm infants.

Method to quantify the shape variability of the central sulcus

Segmentation and reconstruction of whole brains using BrainVISA [1]

Coregistration of the brains in the Talairach space

Extraction of the central sulci

Mirror flip of right central sulci to be aligned with left ones

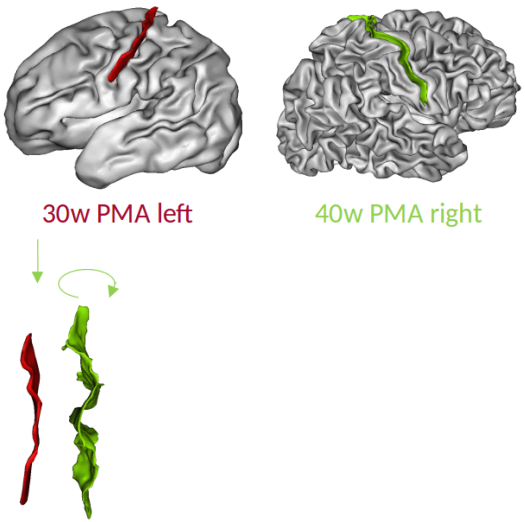

[1] https://brainvisa.info

Method to quantify the shape variability of the central sulcus

Segmentation and reconstruction of whole brains using BrainVISA [1]

Coregistration of the brains in the Talairach space

Extraction of the central sulci

Mirror flip of right central sulci to be aligned with left ones

Pairwise registration of sulci using Iterative Closest Point (ICP)

Residual distance calculation after registration for each pair

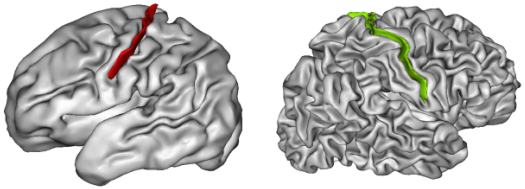

30w PMA left

40w PMA right

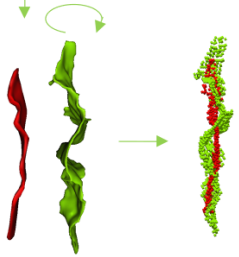

Distance
$d(i, j)$

[1] https://brainvisa.info

Method to quantify the shape variability of the central sulcus

Segmentation and reconstruction of whole brains using BrainVISA [1]

Coregistration of the brains in the Talairach space

Extraction of the central sulci

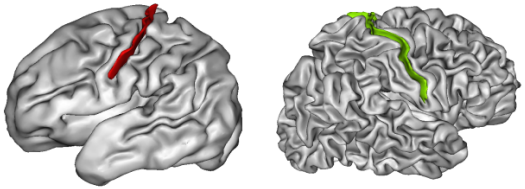

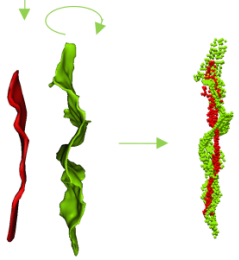

Distance
$d(i, j)$

$$\begin{bmatrix} d(1,1) & \cdots & d(1,284) \\ \vdots & \ddots & \vdots \\ d(284,1) & \cdots & d(284,284) \end{bmatrix}$$

71 subjects x 2 hemispheres x 2 acquisitions

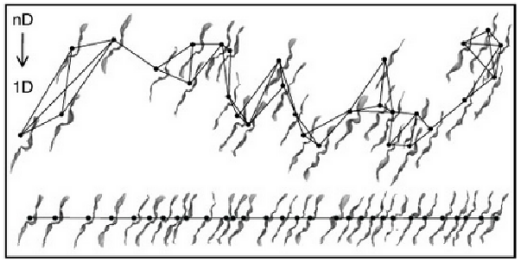

Mirror flip of right central sulci to be aligned with left ones

Pairwise registration of sulci using Iterative Closest Point (ICP)

Residual distance calculation after registration for each pair

Building a high dimension matrix capturing the shape variability of the whole cohort

Dimension reduction Using Isomap to capture The main shape variability

[1] https://brainvisa.info

Example of shape feature captured using this method

→ **The first dimension captures the length and curvature of sulci**

Sulcal projection on the Isomap dimension:

30w PMA
40w PMA

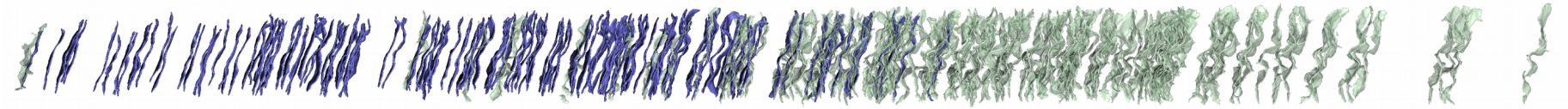

← Short and flat

Long and curvy →

Example of shape feature captured using this method

→ **The first dimension captures the length and curvature of sulci**

Sulcal projection on the Isomap dimension:

30w PMA
40w PMA

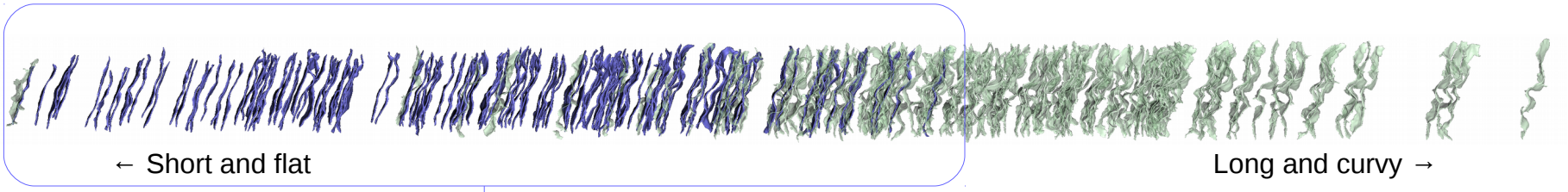

← Short and flat

Long and curvy →

Age-specific moving averages:

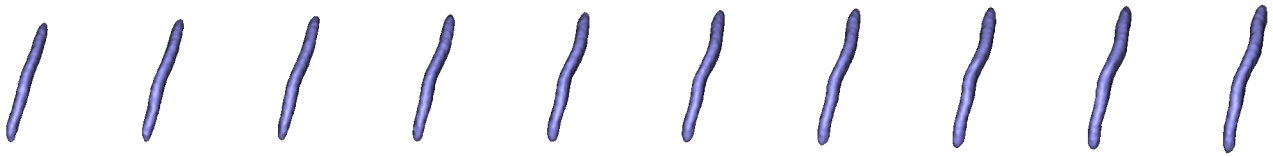

Example of shape feature captured using this method

→ **The first dimension captures the length and curvature of sulci**

Sulcal projection on the Isomap dimension:

30w PMA
40w PMA

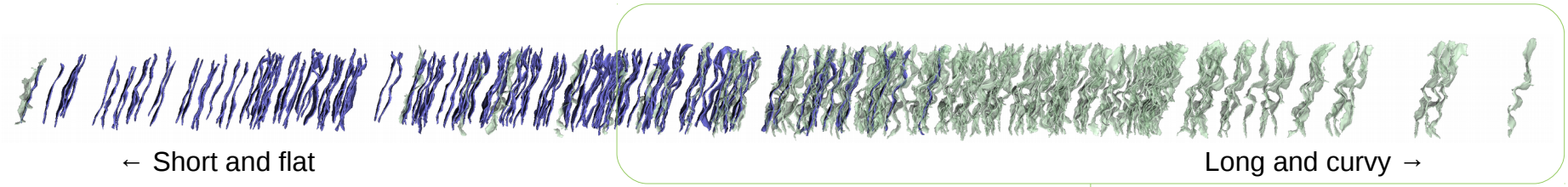

← Short and flat

Long and curvy →

Age-specific moving averages:

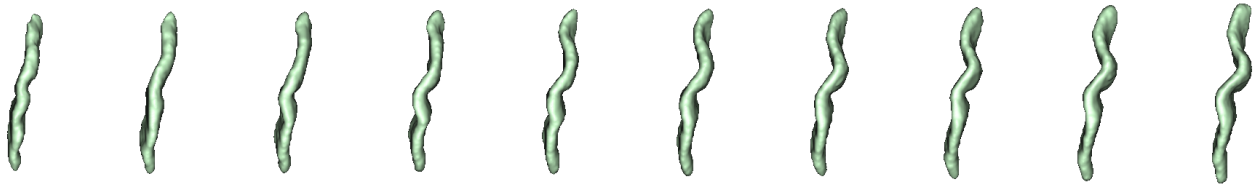

Example of shape feature captured using this method

→ **The first dimension captures the length and curvature of sulci**

Sulcal projection on the Isomap dimension:

30w PMA
40w PMA

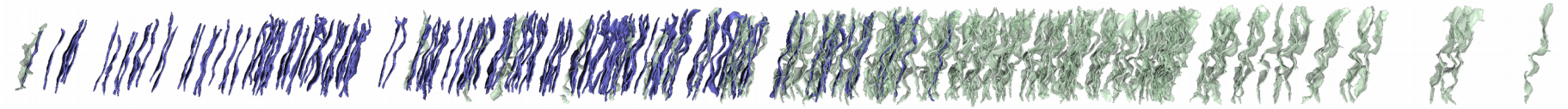

← Short and flat

Long and curvy →

Age-specific moving averages:

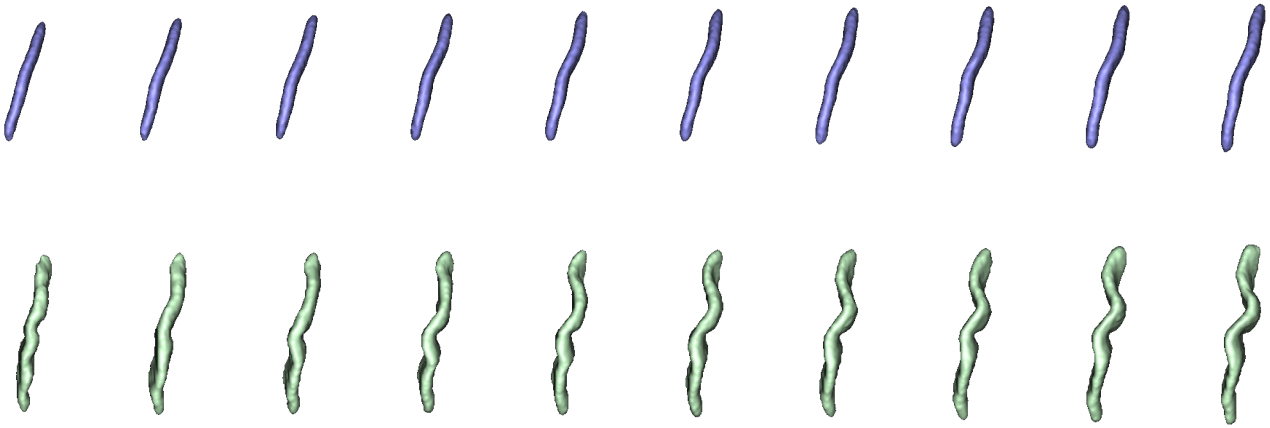

Uses of quantified shape variability

<u>Using raw isomap values:</u>

→ **Description of shape variability in the cohort through visual interpretation**

<u>Using isomap values corrected for PMA at acquisition:</u>
Each analysis is led independently for age and hemisphere subgroups

→ **Shape comparison between 30w and 40w PMA**

→ **Shape comparison between left and right hemispheres**

→ **Motor outcome classification based on shape features** (linear Support Vector Classifier (SVC))

I. Context: why study the developing central sulcus?

II. Method: how to capture the shape variability of the central sulcus?

III. Descriptive results: what shape specificities do we observe in the developing central sulcus?

IV. Predictive results: is the developing central sulcus informative about motor outcome at 5 years?

Longitudinal specificities of the central sulcus

→ **Most of the shape features are consistently encoded between 30w PMA and 40w PMA:** 8/10 dimensions show a relevant trend in Spearman correlations (p-val ≤ 0.05)

→ The shape feature with the most consistent encoding on both sides captured the height and depth of the hand knob, along with the depth of the second knob

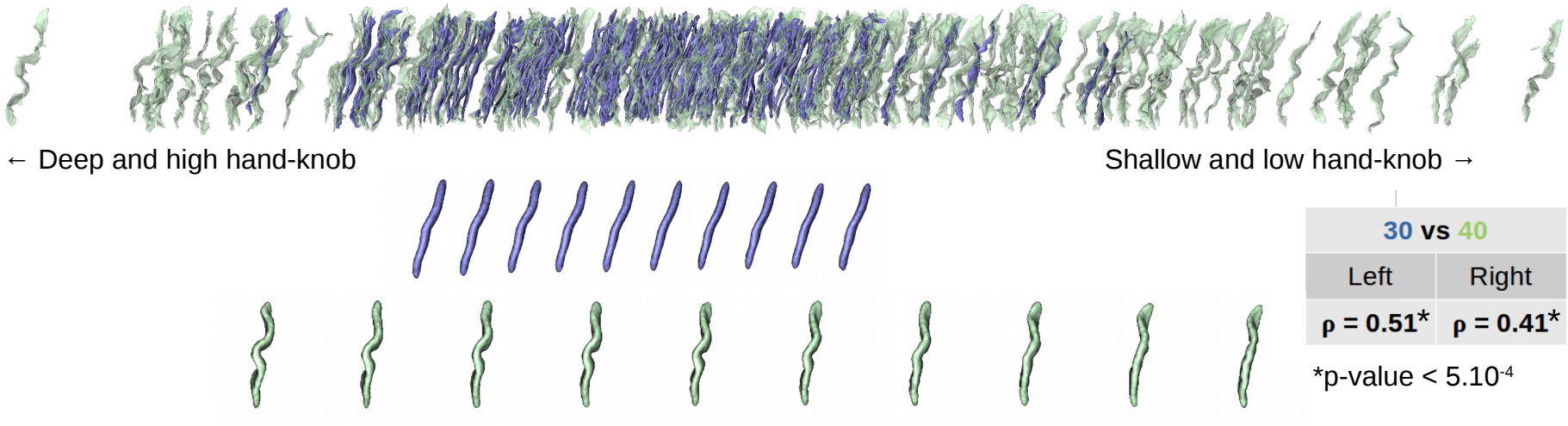

← Deep and high hand-knob

Shallow and low hand-knob →

30 vs 40	
Left	Right
ρ = 0.51*	ρ = 0.41*

*p-value < 5.10^{-4}

Hemispheric specificities of the central sulcus

→ **One shape feature per age group captured a hemispheric asymmetry,** captured with a Wilcoxon signed-rank test.

30w PMA: right central sulci showed a generally lower and deeper hand-knob than left ones

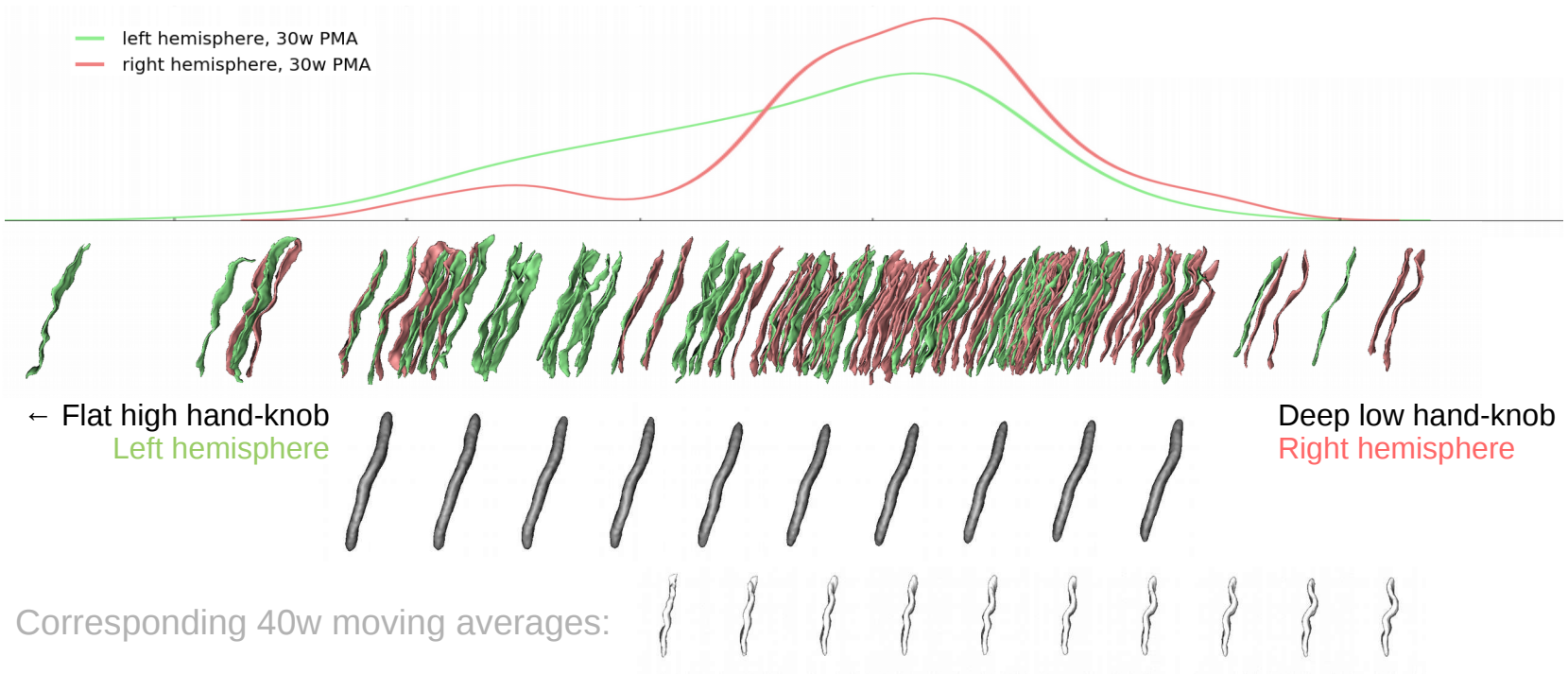

Hemispheric specificities of the central sulcus

→ **One shape feature per age group captured a hemispheric asymmetry,** captured with a Wilcoxon signed-rank test.

40w PMA: right central sulci tended towards a single-knob configuration whereas left ones preferred a double-knob configuration.

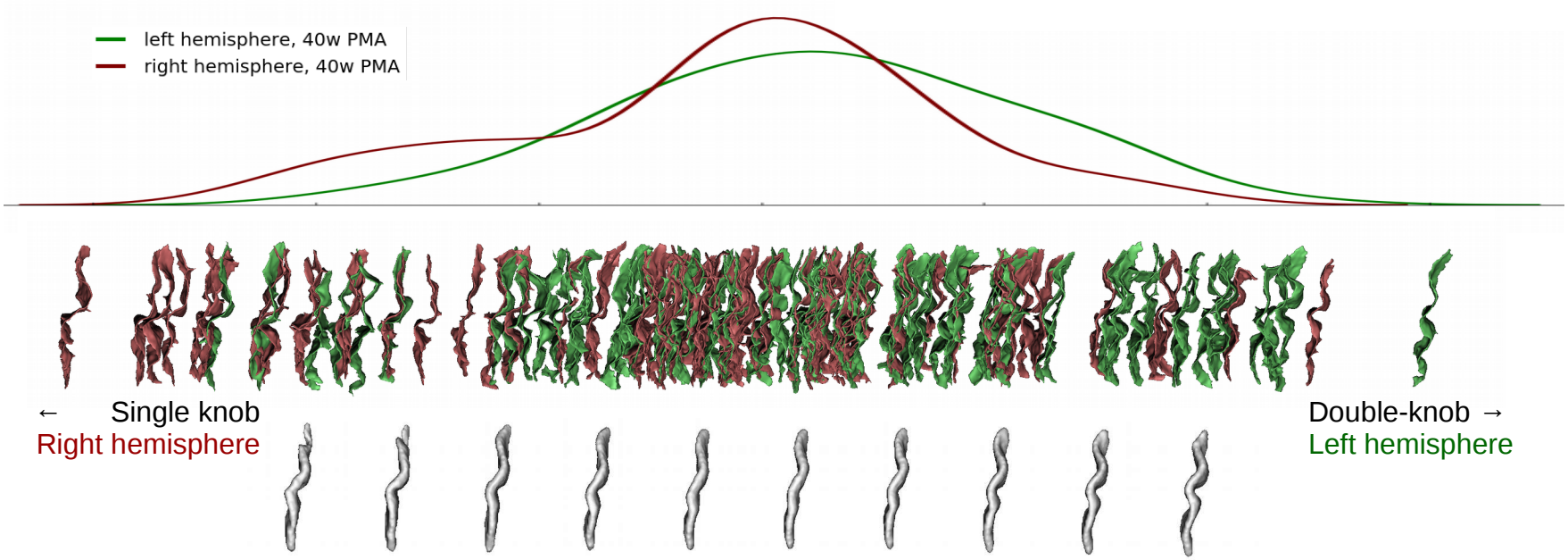

Single to double knob configuration : a trend previously observed in adults

→The asymmetry captured at 40w PMA resembles that previously observed in the adult [1]

Moving averages at 40w PMA

Moving averages in adults

Average shapes on the left hemisphere

Average shapes on the right hemisphere

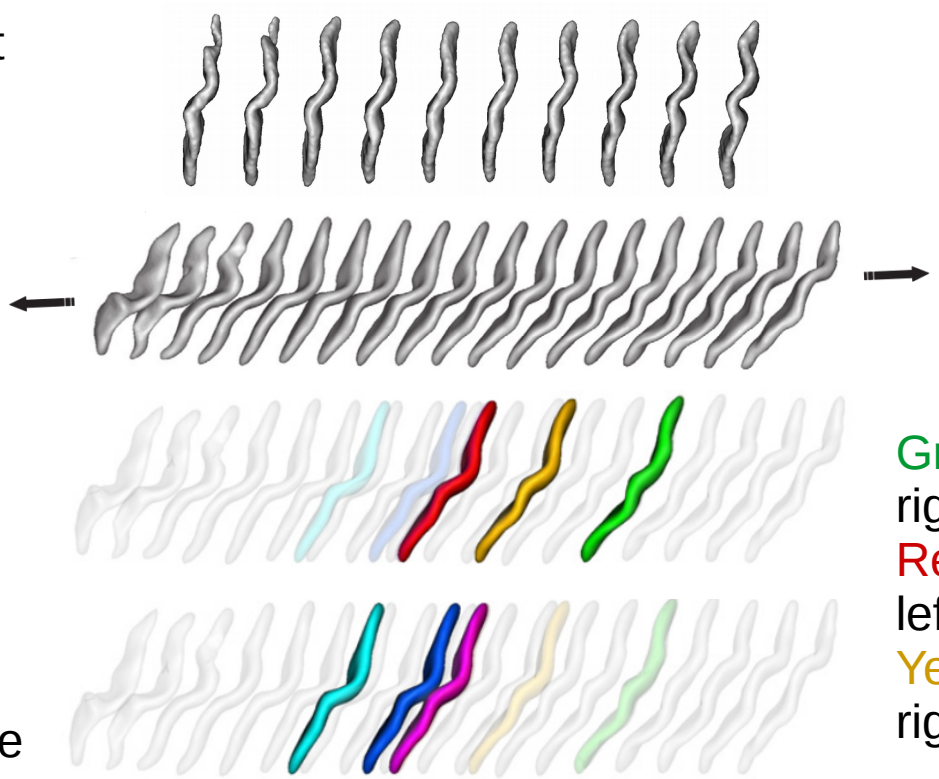

Green/pink: natural right-handers
Red/cyan: natural left-handers
Yellow/blue: forced right-handers

[1] Sun et al., NeuroImage, 2012. The effect of handedness on the shape of the central sulcus.

I. Context: why study the developing central sulcus?

II. Method: how to capture the shape variability of the central sulcus?

III. Descriptive results: what shape specificities do we observe in the developing central sulcus?

IV. Predictive results: is the developing central sulcus informative about motor outcome at 5 years?

Prediction of hand lateralization : method

→ Hand lateralization tested at 5 years

→ Population : **right-handers (n=50)** vs **left-handers with at least one left-handed parent (n=7)**

→ **Method: linear SVC** with a stratified shuffled 5-fold cross-validation repeated 10 times **trained with:**

→ clinical factors alone (gestational age at birth, birth weight z-score, presence of intra-ventricular hemorrhage of grade 3 or 4, and presence of broncho-pulmonar dysplasia)

→ isomap dimensions alone

→ the combination of both

Prediction of hand lateralization : results

→ Using **clinical factors alone**, the area under the receiving operator curve (ROC AUC) was 0.59

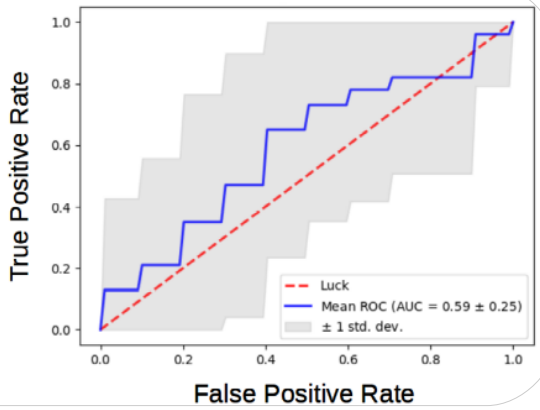

→ The overall best classifier was obtained using **both clinical factors and isomap dimensions** on the **right hemisphere at 30w PMA** (ROC AUC = 0.64)

→ We chose to focus on the best classifier using **isomap dimensions alone,** which was obtained with the **left hemisphere at 30w PMA** (ROC AUC = 0.61)

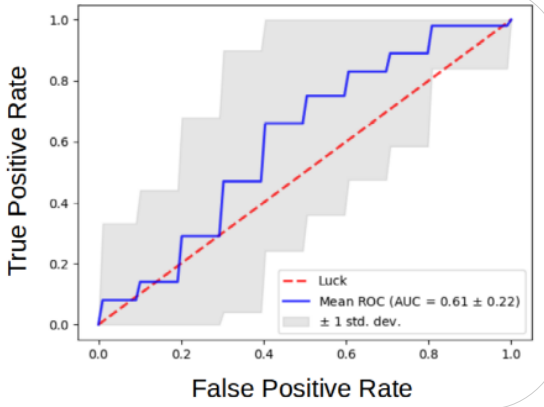

Prediction of hand lateralization : shape analysis

→ On the classifier trained using isomap dimensions alone at 30w PMA, left hemisphere, we retrieved the coefficients assigned to each dimension during the cross-validation

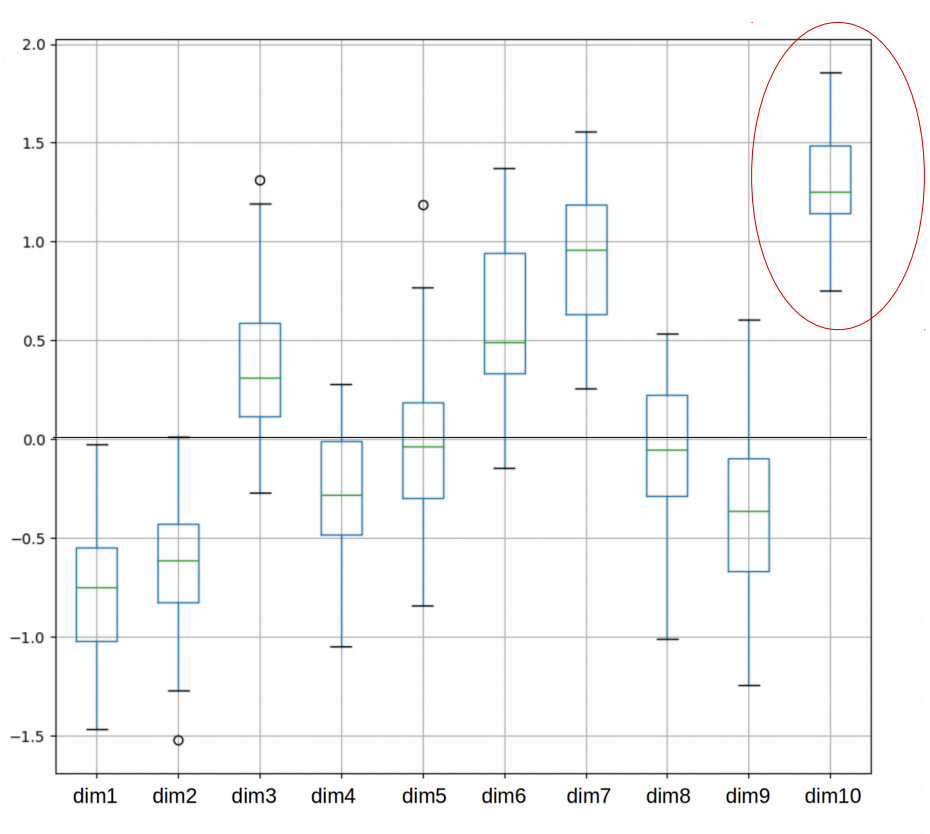

Prediction of hand lateralization : shape analysis

→ **The 10th dimension,** which appeared to be the most informative, **captured the length of the hand knob and the orientation of its upper part**

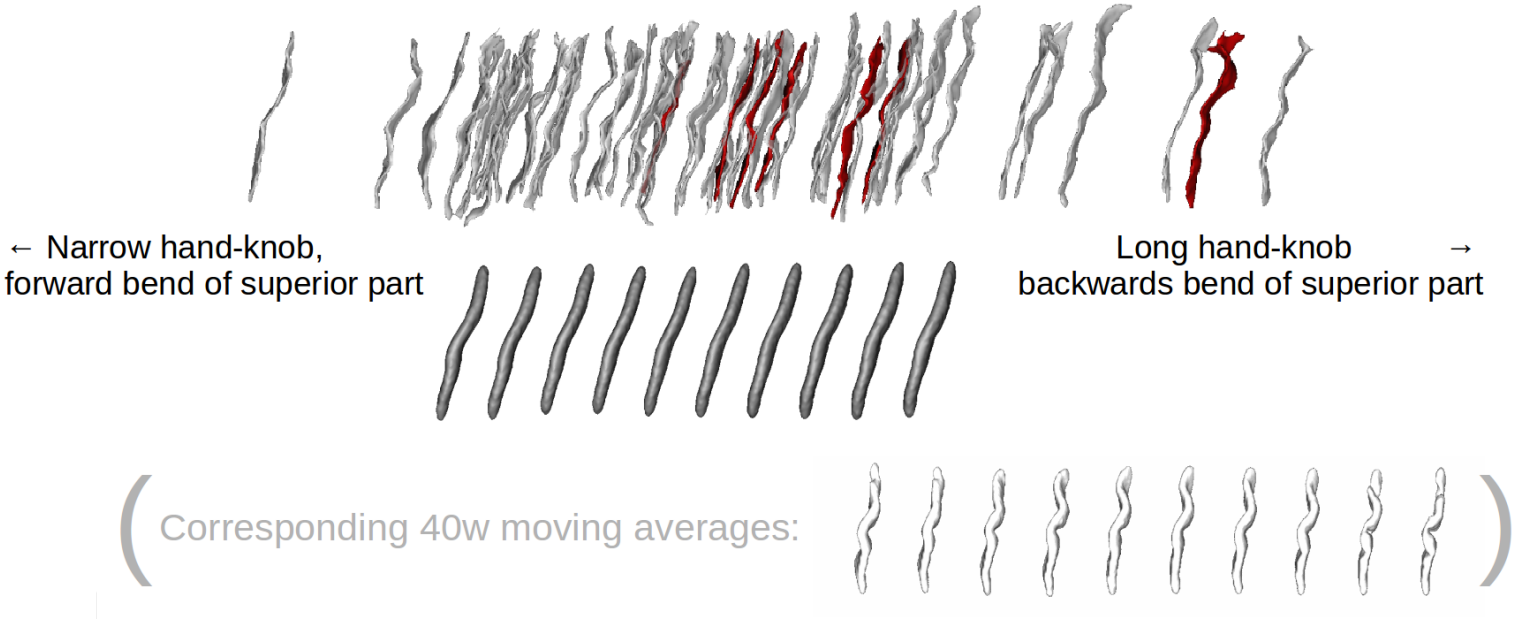

Prediction of fine motor outcome : method

→ Using mABC-II standardized manual dexterity score tested at 5 years.

→ Population: **typical fine motor development (n=35)** vs **poor fine motor development (n=15)**

→ **Method: linear SVC** with a stratified shuffled 5-fold cross-validation repeated 10 times **trained with:**

→ clinical factors alone (gestational age at birth, birth weight z-score, presence of intra-ventricular hemorrhage of grade 3 or 4, and presence of broncho-pulmonar dysplasia)

→ isomap dimensions alone

→ the combination of both

Prediction of fine motor outcome : numerical results

→ Using **clinical factors alone**, the area under the receiving operator curve (ROC AUC) was 0.59

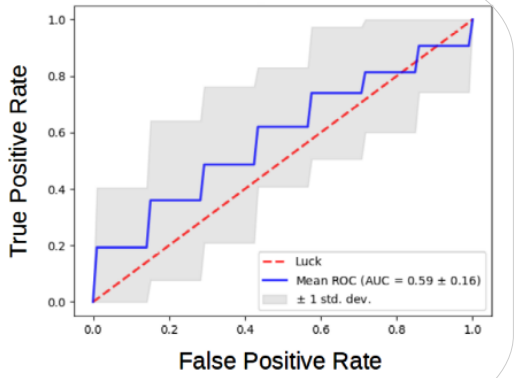

→ Two classifiers scored a tie for the best score. Both used **isomap factors alone**. They were obtained with the **left hemisphere at 30w PMA** and with the **right hemisphere at 40w PMA** (ROC AUCs=0.66)

→ We chose to focus on the **right hemisphere at 40w PMA** because its classifier scored a better recall than the other one (recall = 0.61 vs 0.53)

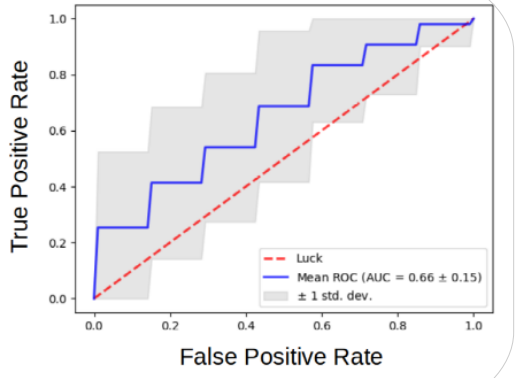

Prediction of fine motor outcome : shape analysis

→ On the classifier trained using isomap dimensions alone at 40w PMA, right hemisphere, dimensions 4 and 10 seemed to be the most informative

Boxplot: coefficients assigned to each dimension during the cross-validation

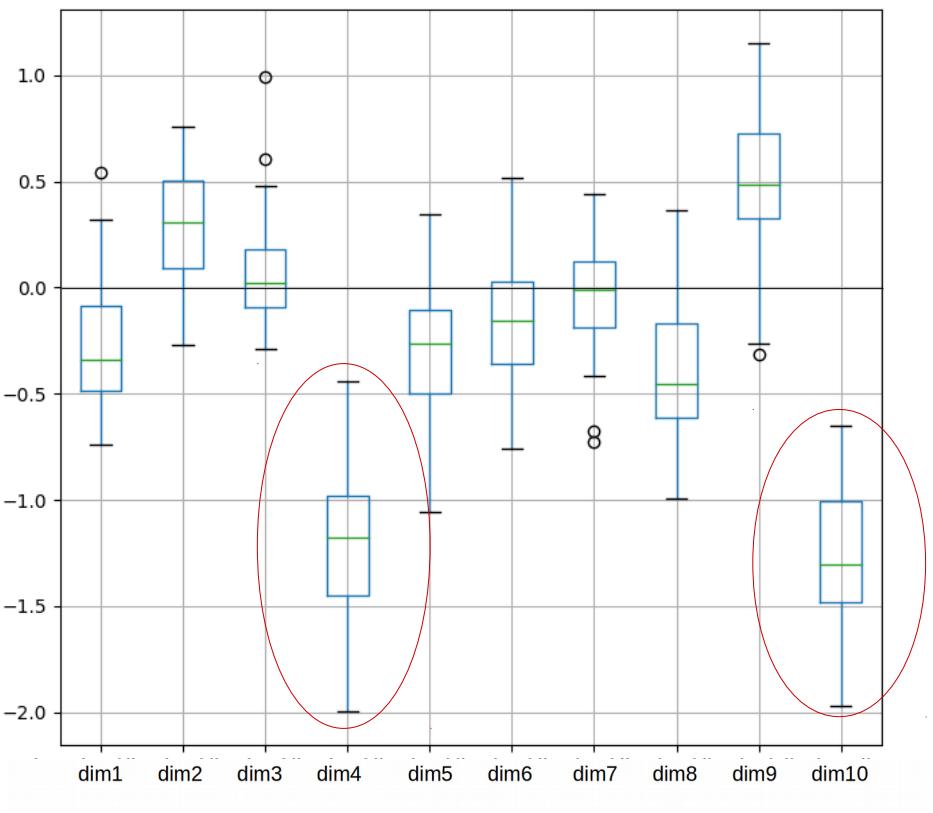

Prediction of fine motor outcome : shape analysis

→ Once again, the **10th dimension** appeared to be the most informative. It **captured the length of the hand knob and the orientation of its upper part**

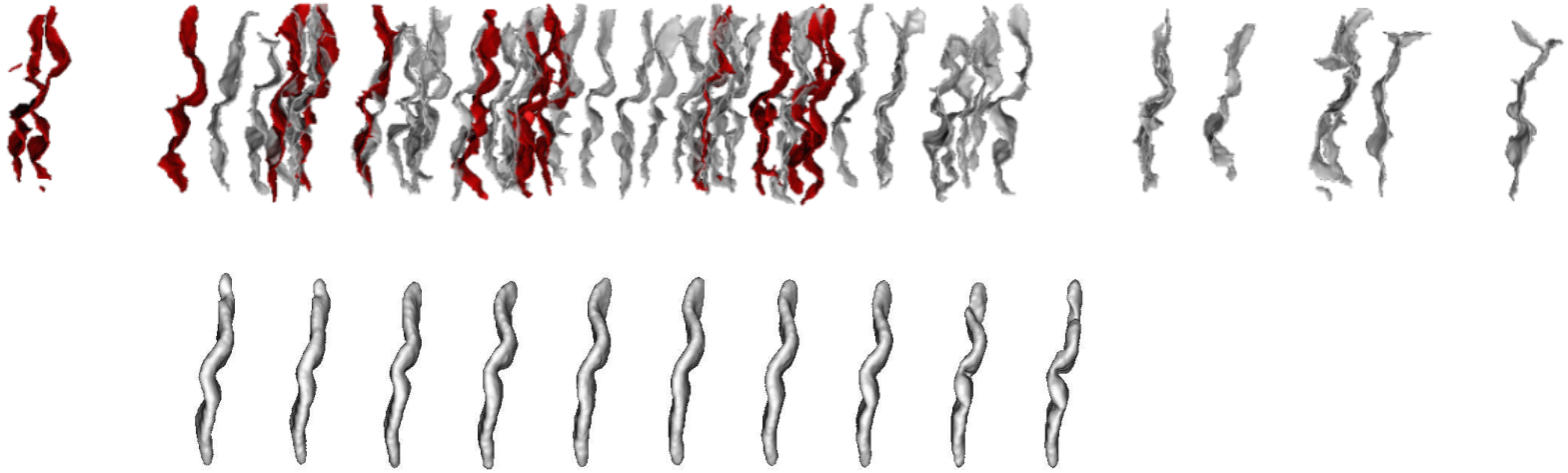

Limitations and perspectives

→ Expectation: **clinical factors** relevant to classify **abnormal fine motor outcome**, and not **lateralization**. Reality: the opposite...

→ The **8th dimension captured in preterms** seems to match the **1st dimension captured in adults** (both in shape and hemispheric asymmetry) ⇒ **this adult feature is already encoded during early development**.

→ Relatively **poor scores** obtained on the outcome classifiers: partly because we **prevented from adjusting the regularization parameter** and **from operating feature selection** because of the size and composition of our dataset.

→ Studying preterms longitudinally: convenient way of looking into the development of sulci, but the results obtained may be linked to **a mix of normal and pathological brain development**.

Take home message:

- We described quantitatively the shape variability of the central sulcus in a very preterm cohort at 30 and 40w PMA

- Most of its early shape features are already encoded as soon as 30w PMA

- Hemispheric asymmetries are already present before normal-term-birth

- The shape of the central sulcus shows a limited but existent predictive capacity on both handedness and fine motor outcome

Thank you for your attention!

Special thanks to my team and partners

Jean-François MANGIN

Jessica DUBOIS

Denis RIVIERE

Clara FISCHER

François LEROY

Joy SUN

Sara Neumann

Manon BENDERS

Linda DE VRIES

Floris GROENENDAAL

Maria-Luisa Tataranno

heloise.devareilles@cea.fr

Annex : detailed description of the cohort

Characteristics	*Mean (range) or N (percentage)*
Perinatal clinical characteristics	
Sex, male	36 (51%)
Gestational age at birth (weeks)	26.5 (24.4 – 27.9)
Birth-weight z-score	0.4 (-2.5 – 1.8)
Presence of severe IVH (grade 3 or 4)	8 (11%)
Presence of broncho-pulmonary dysplasia	20 (39%)
Age at MRI scans	
PMA at early acquisition	30.7 (28.7 – 32.7)
PMA at term-equivalent age acquisition	41.2 (40.0 – 42.7)
Fine motor follow-up at 5-years	
Age at fine motor follow-up	5y9m (4y6m – 6y7m)
Manual lateralization	
Handedness (left / ambidextrous / right) (n=70)	18 / 2 / 50
Corrected handedness* (left / right) (n=57)	7 / 50 (12 / 88%)
Fine motor assessment (n=66)	
mABC manual dexterity standardized score	7.7 (3 – 14)
mABC manual dexterity outcome (poor/borderline/good)	15 / 16 / 35 (23 / 24 / 53%)

*Corrected handedness excludes ambidextrous and left-handed children having both parents right-handed

Annex : focus on the Isomap dimensions (1)

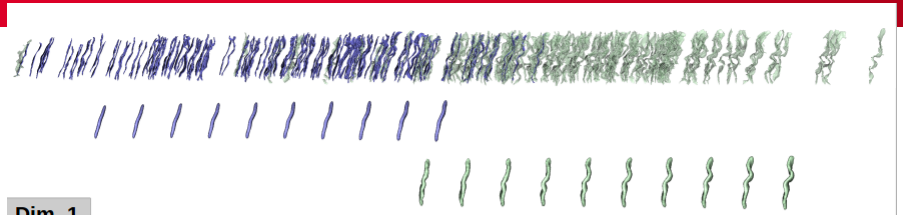

Dim. 1

Length and curvature
From short and flat sulci on the left to long and curvy sulci on the right

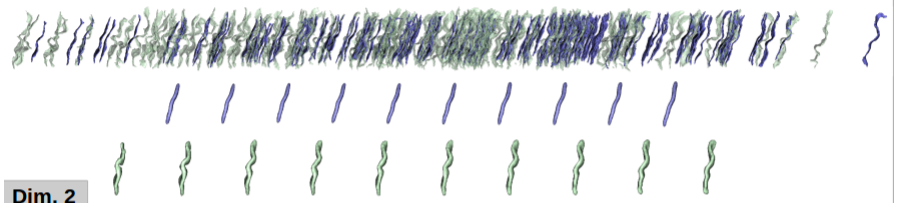

Dim. 2

Height of the hand knob and depth of the second knob
From sulci with high hand-knobs and deep second-knobs on the left to sulci with low hand-knobs and shallow second-knobs on the right

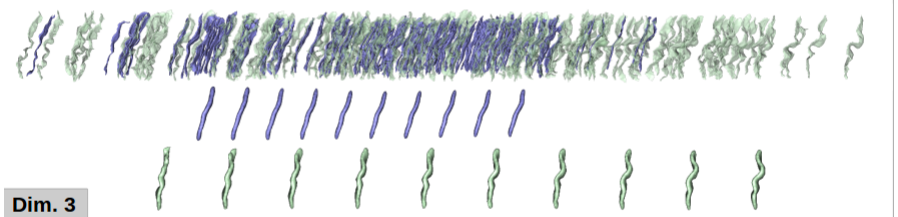

Dim. 3

Curvature of the hand-knob at fixed height
From sulci with flatter or poorly-defined hand-knobs on the left to sulci with deep hand-knobs on the right, with no height shift of the hand-knob along the axis.

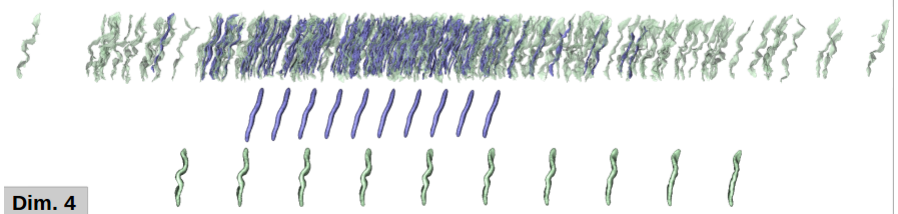

Dim. 4

Depth and height of the hand knob, depth of second knob
From sulci with deeper and higher hand-knobs on the left to sulci with shallower and lower hand-knobs on the right. Note that the second knob, deep on the left, fades out along the axis.

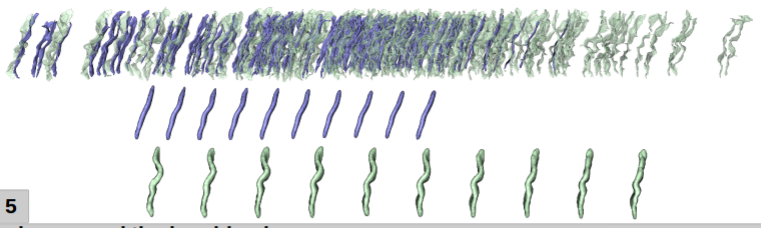

Dim. 5

Wrapping around the hand-knob
From sulci with wrapped-around hand-knobs on the left to sulci with open hand-knobs on the right

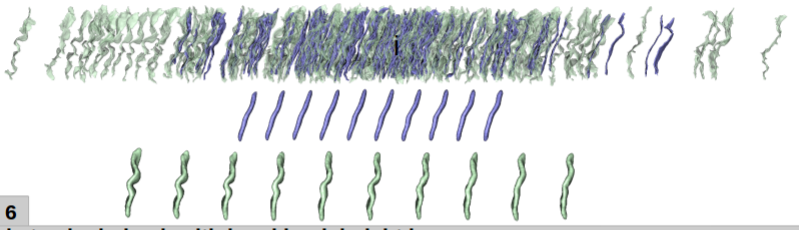

Dim. 6

Double to single-knob with hand-knob height increase
From sulci with two knobs and a lower hand-knob on the left to sulci with a single-knob configuration on the right, with a higher hand-knob

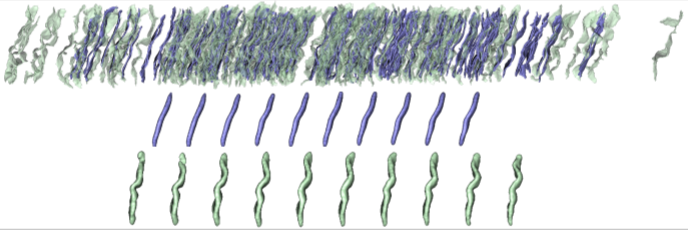

Dim. 7

Height of the hand-knob at fixed depth
From sulci with wrapped-around hand-knobs on the left to sulci with open hand-knobs on the right

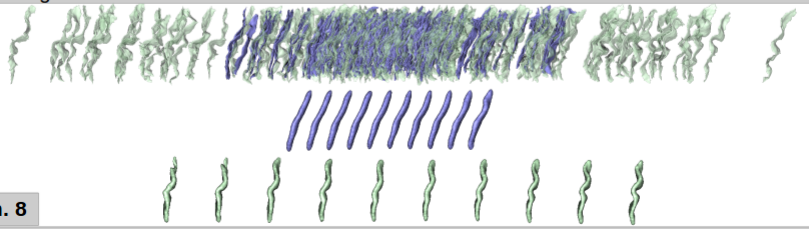

Dim. 8

Single to double-knob with hand-knob height increase
From sulci with a single-knob configuration and a lower hand-knob to sulci with a double-knob configuration and a higher hand-knob

Annex : focus on the Isomap dimensions (2)

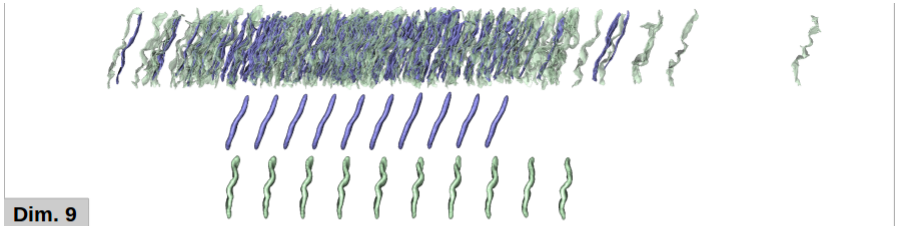

Dim. 9

Upper orientation of the sulcus
From sulci with the upper part bending backward (towards somatosensory region) on the left to sulci with the upper part bending forward (toward motor region) on the right

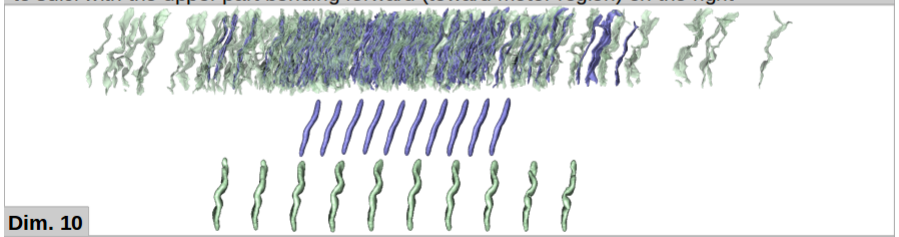

Dim. 10

Width of the hand-knob
From sulci with a shorter hand-knob on the left to sulci with a longer hand-knob on the right, with no depth, wrapping nor height shift of the hand knob along the axis.

Annex : Classifier scores for handedness

	subgroup	Balanced accuracy	ROC AUC
1) Baseline: clinical factors alone		0.55	0.59
2) Sulcal shape alone	Left hemisphere, 30w PMA	**0.57**	**0.61**
	Right hemisphere, 30w PMA	0.38	0.35
	Left hemisphere, 40w PMA	0.44	0.49
	Right hemisphere, 40w PMA	0.43	0.33
3) Combination of sulcal shape and clinical factors	Left hemisphere, 30w PMA	0.53	**0.65**
	Right hemisphere, 30w PMA	**0.64**	**0.65**
	Left hemisphere, 40w PMA	0.48	0.57
	Right hemisphere, 40w PMA	0.43	0.37

Annex : Classifier scores for fine motor outcome

	subgroup	Balanced accuracy	ROC AUC
1) Baseline: clinical factors alone		0.58	0.59
2) Sulcal shape alone	Left hemisphere, 30w PMA	**0.62**	**0.66**
	Right hemisphere, 30w PMA	0.45	0.44
	Left hemisphere, 40w PMA	0.40	0.38
	Right hemisphere, 40w PMA	**0.62**	**0.66**
3) Combination of sulcal shape and clinical factors	Left hemisphere, 30w PMA	**0.59**	**0.61**
	Right hemisphere, 30w PMA	0.48	0.50
	Left hemisphere, 40w PMA	0.46	0.41
	Right hemisphere, 40w PMA	0.57	**0.64**

Annex : focus on recall

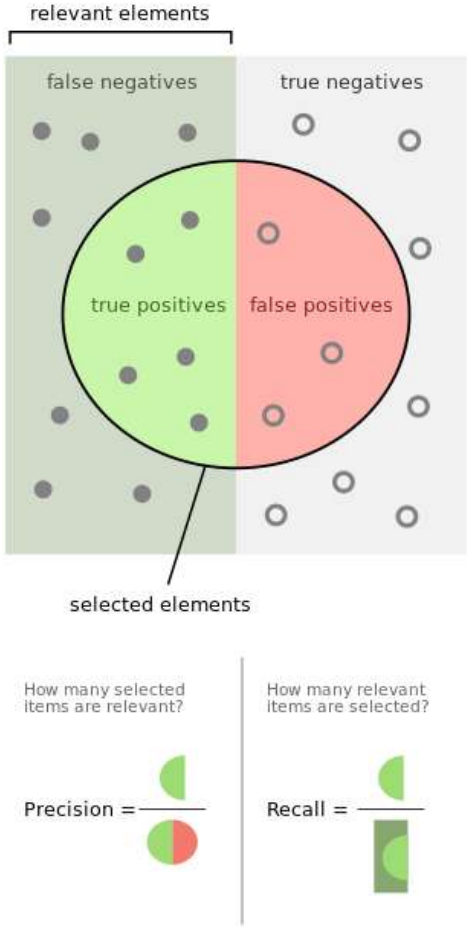

Recall: proportion of elements correctly identified as positive relative to the total number of positives

=> by considering recall, we value the fact of identifying a big proportion of the positive class, even if it means capturing false positives.

Image from the wikipedia page “precision and recall”

Annex : Full statistics tables

	Wilcoxon signed-rank test: t (p-value)			
	A. Hemispheric comparison		B. Age-group comparison	
	L30 vs R30	L40 vs R40	L30 vs L40	R30 vs R40
Dimension 1	959 (0.068)	1022 (0.142)	**3.0 (3.10^{-13})**	**0.0 (2.10^{-13})**
Dimension 2	1044 (0.180)	1276 (0.991)	882.0 (0.023)	**774.0 (0.004)**
Dimension 3	**757 (0.003)**	1110 (0.336)	903.0 (0.032)	978.0 (0.086)
Dimension 4	941 (0.053)	1113 (0.344)	**627.0 (2.10^{-4})**	1129.0 (0.393)
Dimension 5	878 (0.022)	1137 (0.419)	**606.0 (1.10^{-4})**	**686.0 (7.10^{-4})**
Dimension 6	1133 (0.406)	1152 (0.470)	1165.0 (0.517)	1178.0 (0.567)
Dimension 7	1169 (0.532)	947 (0.058)	986.0 (0.094)	849.0 (0.014)
Dimension 8	1242 (0.837)	**775 (0.004)**	804.0 (0.007)	1138.0 (0.422)
Dimension 9	1208 (0.689)	1254 (0.891)	1099.0 (0.305)	1212.0 (0.705)
Dimension 10	1132 (0.403)	881 (0.023)	871.0 (0.020)	1066.0 (0.224)

	Spearman correlation: ρ (p-value)			
	A. Hemispheric comparison		B. Age-group comparison	
	L30 vs R30	L40 vs R40	L30 vs L40	R30 vs R40
Dimension 1	**0.607 (2.10^{-8})**	**0.385 (9.10^{-4})**	0.232 (0.051)	**0.428 (2.10^{-4})**
Dimension 2	**0.407 (4.10^{-4})**	0.232 (0.051)	**0.458 (6.10^{-5})**	0.329 (0.005)
Dimension 3	0.222 (0.063)	**0.351 (0.003)**	0.307 (0.009)	**0.353 (0.003)**
Dimension 4	0.254 (0.032)	0.283 (0.017)	**0.512 (5.10^{-6})**	**0.414 (3.10^{-4})**
Dimension 5	**0.411 (3.10^{-4})**	0.327 (0.005)	**0.376 (0.001)**	0.317 (0.007)
Dimension 6	0.216 (0.070)	0.150 (0.213)	0.284 (0.017)	**0.383 (0.001)**
Dimension 7	0.188 (0.116)	0.249 (0.036)	0.081 (0.500)	0.191 (0.111)
Dimension 8	0.212 (0.076)	0.186 (0.120)	0.246 (0.039)	**0.522 (3.10^{-6})**
Dimension 9	0.157 (0.190)	0.123 (0.308)	0.294 (0.013)	**0.334 (0.004)**
Dimension 10	0.158 (0.189)	0.264 (0.026)	-0.024 (0.842)	-0.063 (0.599)

Annex : Image preprocessing

MRI acquisition: 3-Tesla MR system (Achieva, Philips Medical Systems, Best, The Netherlands).
The protocol included T2-weighted imaging with a turbo-spin echo sequence in the coronal plane (at early MRI: repetition time (TR) 10.085 ms; echo time (TE) 120 ms; slice thickness 2 mm, in-plane spatial resolution 0.35 × 0.35 mm; at TEA: TR 4847 ms; TE 150 ms; slice thickness 1.2 mm, in-plane spatial resolution 0.35 × 0.35 mm).
Data preprocessing: after generating a brain mask, T2-weighted images were segmented into three classes between grey matter, unmyelinated white matter and cerebrospinal fluid using supervised voxel classification. By adapting the BabySeg and Morphologist anatomical pipelines of the BrainVISA software, these segmentations allowed a reconstruction of the inner cortical surfaces of both hemispheres, and the extraction of objects depicting the sulci.

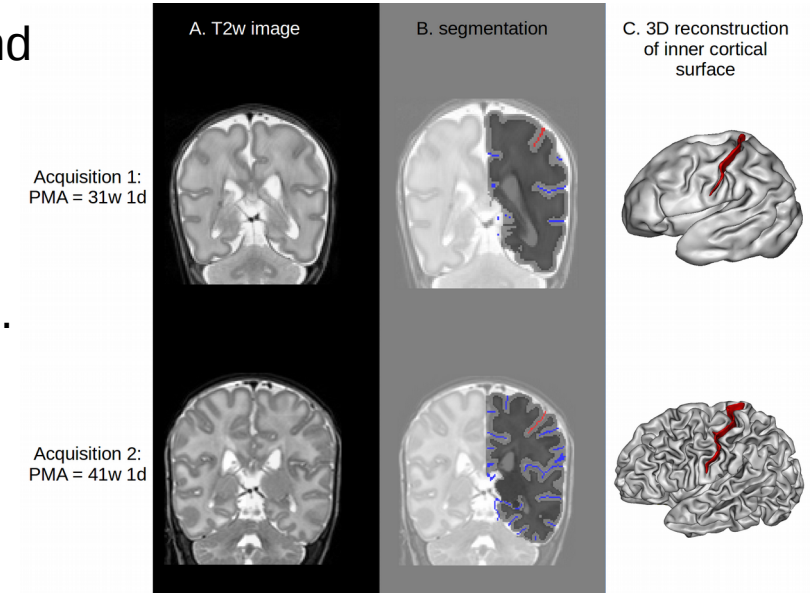

Annex : parameter selection for isomap

1) Compute intrinsic dimensionality d_int of the manifold for each possible number of nearest neighbors k by maximizing the ratio of the reconstruction error a randomly generated distance matrix with the reconstruction error of the input matrix
2) Using the couple {k, d_opt}, compute the reconstruction error depending on k
3) Look for error drop and check the extent in which the choice of k in this range affects the results
4) Select k in this range using the plot of residual variance based on k
5) Choose the most interesting number of dimensions d_opt to observe based on the relative increase of the reconstruction error ratio with increasing dimension

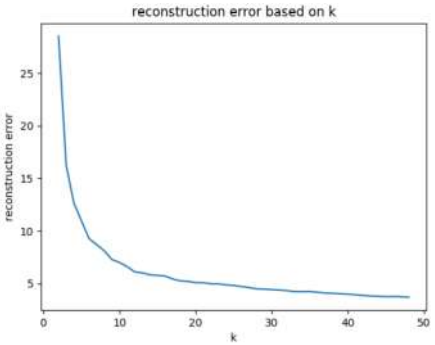

A. step 2

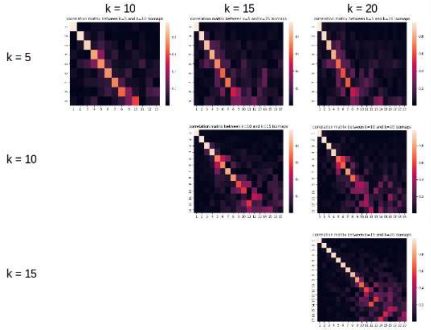

B. step 3

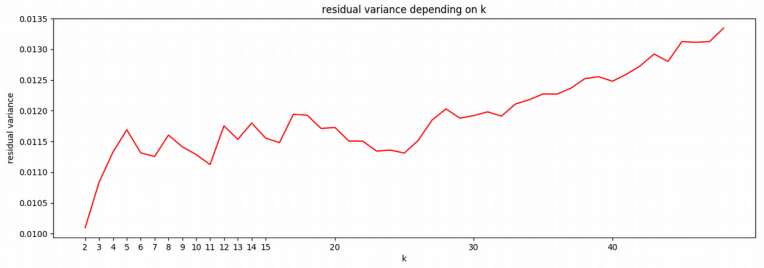

C. step 4

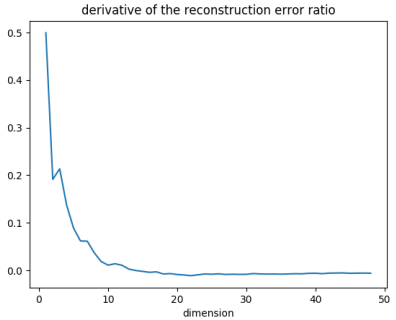

D. step 5

Result: k_opt=11, d_opt=10